ARTICLE
Journal of Cellular Biochemistry 114:1843–1851 (2013)

Journal of Cellular Biochemistry

Knock Down of Caveolin-1 Affects Morphological and Functional Hallmarks of Human Endothelial Cells

Luca Madaro,[1] Fabrizio Antonangeli,[1,2] Annarita Favia,[1] Bianca Esposito,[1] Filippo Biamonte,[3] Marina Bouché,[1] Elio Ziparo,[1] Gigliola Sica,[3] Antonio Filippini,[1] and Alessio D'Alessio[3*]

[1] *Department of Anatomy, Histology, Forensic Medicine and Orthopedics, Section of Histology and Medical Embryology, Sapienza University of Rome, Rome, Italy*

[2] *Faculty of Life Sciences, University of Manchester, Oxford Road, M13 9PT, Manchester, UK*

[3] *Institute of Histology and Embryology, Faculty of Medicine, Catholic University of the Sacred Heart, Rome, Italy*

ABSTRACT

Caveolin-1 (CAV1) is the principal structural component of caveolae which functions as scaffolding protein for the integration of a variety of signaling pathways. In this study, we investigated the involvement of CAV1 in endothelial cell (EC) functions and show that siRNA-induced CAV1 silencing in the human EC line EA.hy926 induces distinctive morphological changes, such as a marked increase in cell size and formation of stress fibers. Design-based stereology was employed in this work to make unbiased quantification of morphometric properties such as volume, length, and surface of CAV1 silenced versus control cells. In addition, we showed that downregulation of CAV1 affects cell cycle progression at G1/S phase transition most likely by perturbation of AKT signaling. With the aim to assess the contribution of CAV1 to typical biological processes of EC, we report here that CAV1 targeting affects cell migration and matrix metalloproteinases (MMPs) activity, and reduces angiogenesis in response to VEGF, in vitro. Taken together our data suggest that the proper expression of CAV1 is important not only for maintaining the appropriate morphology and size of ECs but it might represent a prospective molecular target for studying key biological mechanisms such as senescence and tumorigenesis. J. Cell. Biochem. 114: 1843–1851, 2013.

KEY WORDS: CAVEOLIN-1; ANGIOGENESIS; MMP; STEREOLOGY; ENDOTHELIAL CELLS

Caveolins are a family of small trans-membrane proteins which include caveolin-1 (CAV1), caveolin-2 (CAV2), and caveolin-3 (CAV3) [Glenney and Soppet, 1992; Scherer et al., 1996; Song et al., 1996; Gazzerro et al., 2010]. All caveolins form a hairpin structure that crosses the plasma membrane with the N- and C-terminus domain of the protein facing the cytoplasm. Caveolins are usually found in the majority of mammalian adherent cells, where CAV1 and -2 are mainly expressed in endothelial cells (ECs) and adipocytes [Hansen and Nichols, 2010] while CAV3 is referred to as muscle specific, being restricted to skeletal, smooth, and cardiac muscle [Gazzerro et al., 2010]. The ability of CAV1 to form homooligomers and heterooligomers with CAV2, typically in the endoplasmic reticulum (ER), and their high affinity for cholesterol and glycosphingolipids are crucial for the insertion of the protein into the plasma membrane and for the formation of flask-like invaginations called caveolae [Thiele et al., 2000; Sengupta, 2012], small non-clathrin coated invaginations found in many cell types [Parton and Simons, 2007]. Caveolae have been thought for long time to be only involved in the endocytic pathways and membrane trafficking and only more recently their contribution to multiple pathways [Chidlow and Sessa, 2010] such as ETB-induced calcium signaling [Gambara et al., 2008], leukocyte extravasation [Reglero-Real et al., 2012], regulation of cellular homeostasis and tumorigenesis has been demonstrated [Parton and Simons, 2007; Burgermeister et al., 2008; Fernandez-Rojo et al., 2012]. The contribution of CAV1 to cell proliferation is a matter of debate and a number of studies have generated conflicting data. Expression of CAV1 has been also associated to tumor progression and survival

The authors have no financial conflicts of interest.

Luca Madaro and Fabrizio Antonangeli contributed equally to this work.

Grant sponsor: Ministero dell'Università e della Ricerca (MIUR); Grant sponsor: Fondazione Roma.

*Correspondence to: Alessio D'Alessio, Institute of Histology and Embryology, Catholic University of the Sacred Heart School of Medicine, Largo Francesco Vito 1, 00168 Rome, Italy. E-mail: alessio.dalessio@rm.unicatt.it

Manuscript Received: 22 January 2013; Manuscript Accepted: 21 February 2013

Accepted manuscript online in Wiley Online Library (wileyonlinelibrary.com): 5 March 2013

DOI 10.1002/jcb.24526 • © 2013 Wiley Periodicals, Inc.

[Quest et al., 2012], suggesting that this protein regulates disparate cellular functions most likely activating cell-specific signaling pathways. In different tumor cell types, CAV1 usually appears downregulated or inactivated [Bai et al., 2012; Roy et al., 2012]. CAV1 may function to keep key molecules into definite cellular compartments, like caveolae or lipid rafts, facilitating protein–protein interaction [D'Alessio et al., 2005]. ECs activation [Pober and Sessa, 2007], recruitment of matrix metalloproteinases (MMPs) and the degradation of the basal lamina (BL) are essential steps to achieve angiogenesis, which is regulated by specific molecules such as the vascular endothelial growth factor (VEGF) and basic fibroblast growth factor (bFGF) and counteracted by a number of angiogenesis inhibitor [Kerbel and Folkman, 2002] or by the family of tissue inhibitors of metalloproteinases (TIMPs) [Newby, 2012], which act by degrading specific components of the extracellular matrix (ECM) [Stetler-Stevenson, 1999] promoting cell proliferation and invasion. Our group and others have been studying the contribution of CAV1 to EC functions such as TNF-induced signaling in different EC types such as HUVEC and EA.hy926 line [Feng et al., 2001; D'Alessio et al., 2005, 2010]. In this work, we further characterized CAV1 functions in human EC by showing that the genetic silencing of the CAV1 induced changes in cell morphology and arrested cell cycle at G1/S phase transition. Finally, we demonstrated that CAV1 significantly contributed to the regulation of MMPs activity, which influences both EC migration and the formation of new blood vessels, indicating a role of caveolin in regulating cell growth and angiogenesis.

MATERIALS AND METHODS

CELL CULTURE AND REAGENTS

The human-derived EA.hy926 EC line [Edgell et al., 1983] was kindly donated by Dr. William Sessa (Yale University School of Medicine) and maintained in Dulbecco's modified Eagle's medium (Life Technologies Corporation) containing 10% (v/v) fetal calf serum, 2% (w/v) HAT (hypoxanthine/aminopterin/thymidine) (Sigma), 200 μM L-glutamine, 100 units/ml penicillin/streptomycin (Life Technologies) at 37°C in a 5% CO_2 humidified atmosphere. Mouse anti-human CAV1 antibody was from BD Biosciences (Bedford). Rabbit anti-cyclin-D1, rabbit anti-pERK, rabbit anti-phospho-AKT, anti-AKT, and LY294002 were from Cell Signaling Technology. Horseradish peroxidase (HRP)-conjugated secondary antibodies and SuperSignal West Pico Chemoluminescent substrate (ECL) were from Pierce. Oligofectamine was purchased from Life Technologies Corporation. $VEGF_{165}$ was from Peprotech. FAK inhibitor 14 was purchased from Santa Cruz. All other reagents were purchased from Sigma.

QUANTITATIVE REAL-TIME PCR ANALYSIS

For real-time PCR analysis total RNA was extracted with the TRIZOL Reagent (Life Technologies Corporation), according to the manufacturer's instructions. In brief, 3 μg of RNA were retro-transcribed into single-stranded DNA by a standard 20 μl RT reaction with the TaqMan RT Reagent (Life Technologies Corporation). Real-time quantitative RT-PCR was performed using the 7500 Real-Time PCR System (Life Technologies Corporation). cDNA generated from the reverse transcription reactions was amplified by PCR with the SensiMix SYBR kit (Bioline) in a total volume of 25 μl according to the manufacturer's instructions. The primers used were as follows: CAV1, 5′-AAGATTTTCTTCCTTCCTCAGTTCCCTTA-3′ and 5′-CCC-GTGGCTGGATGAAAAC-3′, and β-actin, 5′-TGCACCACACCTT-CTACAATGA-3′ and 5′-CAGCCTGGATAGCAACGTACAT-3′. The level of gene expression was expressed as relative fold change versus the β-actin messenger RNA using the $\Delta\Delta C_t$ method [Livak and Schmittgen, 2001] using the 7500 System Software (Life Technologies Corporation).

SMALL INTERFERING RNA EXPERIMENTS

Small interfering RNA duplex oligonucleotides complementary to the coding sequence of human CAV1 cDNA (NM_001753) were synthesized and purchased by Integrated DNA Technologies as previously described [D'Alessio et al., 2010]. Non-targeting siRNA used as a negative control for evaluating RNAi off-target effects was from Santa Cruz. Transfection of 10 nM siRNA in EA.hy926 was carried out with Oligofectamine Transfection Reagent, according to the manufacturer's instructions. Complete fresh medium was added 6 h after transfection and cells were further incubated for 72 h prior to proceed with other treatments. Commercial non-targeting control siRNA-A (Santa Cruz) served as experimental control.

SDS–PAGE AND WESTERN BLOT ANALYSIS

After treatments ECs were washed twice in ice-cold phosphate-buffered saline (PBS) and left in a lysis buffer containing 20 mM Tris–HCl pH 7.5, 150 mM NaCl, 1 mM Na_2EDTA, 1 mM EGTA, 1% Triton, 2.5 mM sodium pyrophosphate, 1 mM β-glycerophosphate, 1 mM Na_3VO_4, 1 μg/ml leupeptin, 2% SDS, and 1 mM Pefabloc for 15 min on ice. Total cell lysate was cleared by centrifugation at 12,000*g* for 10 min at 4°C. Proteins content was measured with the BCA Protein Assay Reagent (Thermo Fisher Scientific, Inc.) and equal amount of proteins was separated by SDS–PAGE, transferred to a nitrocellulose membrane (Bio-Rad) and subjected to immunoblotting. Detection of the bound primary antibody was performed by enhanced chemiluminescence (Thermo Fisher Scientific, Inc.). Intensities of immunoblotted bands were measured and normalized to the intensity of the band for β-actin with the Scion Image Application Software Ver. 1.45s (Scion Corporation).

ANALYSIS OF CELL CYCLE

For cell cycle analysis cells were harvested by trypsin and fixed overnight with 75% ethanol at 4°C. After fixing, cells were washed with HBSS containing 1% BSA and incubated with a PBS buffer containing 50 μg/ml propidium iodide (PI) and 100 U/ml of RNAse/DNAse for 2 h at room temperature. Cells were then analyzed using a Coulter Epics XL flow cytometer (Beckman Coulter) and cell cycle distribution was analyzed using the WinMDI 2.8 software (Scripps Research Institute).

EVALUATION OF CELL MIGRATION AND MONOLAYER SCRATCH ASSAY

Cell migration was evaluated by Boyden chamber assay with matrix-coated membranes with 8 μm pore size (BD Biosciences). The chamber was prepared with medium containing 5% serum in the lower well. After pH equilibration in a 5% CO_2-containing

atmosphere, a suspension of 150,000 cells was added to the upper wells of the chambers. Migration was allowed to proceed for 24 h. The membrane was washed in PBS and the cells remaining in the upper face of the membrane were scraped. The membrane was then fixed in 100% ethanol for five min and rinsed in water. The membrane was stained with hematoxylin and cells were counted under a microscope. For monolayer scratch assay [Liang et al., 2007] confluent EC monolayers plated onto 35 mm dishes were scraped in a straight line with a p200 pipet tip to create a "scratch" of similar size in both the control and CAV1 silenced cells. After removing debris by gentle washing of cells, fresh medium with or without 100 ng/ml VEGF was added to the culture for the indicated times. Cells were analyzed with an inverted microscopy equipped with a digital camera.

TUBE FORMATION ASSAY

Tube formation was evaluated by angiogenesis in vitro assay. Briefly, 130 μl of Matrigel Basement Membrane Matrix (BD Biosciences) was left to solidify onto pre-cooled 48-well tissue culture at 37°C for 60 min. Then, 40,000 cells in a final volume of 500 μl were seeded onto the surface of each well containing the polymerized matrix and stimulated with 100 ng/ml VEGFA165 (Peprotech) for additional 24 h at 37°C. Tube formation was evaluated under an inverted microscope (Nikon Eclipse TS100) at 20× magnification and images were acquired by a digital camera (Nikon Coolpix995). In some experiments, was employed the "In vitro Angiogenesis Assay Kit" (Cayman Chemical Company). Briefly, 1×10^4 control or CAV1 silenced cells were cultured in the presence of stimulators of angiogenesis or with vehicle alone for 20 h at 37°C. Cells were then stained with calcein-AM and examined under an inverted fluorescence microscope.

GELATIN ZYMOGRAPHY

The MMP-2 activity in the conditioned media and in the cells was quantified separately by gelatin-substrate zymography. After transfection of CAV1 siRNA or control siRNA, an equal amount of proteins from cell-conditioned medium and cell lysates were separated on 8% SDS–PAGE containing 1 mg/ml (final concentration) gelatin B under non-reducing conditions. Electrophoresis was performed in non-reducing conditions, and SDS was removed by incubating the gel in 2% Triton X-100 at 37°C for 30 min. The gel was then soaked in 0.05 M Tris–HCl buffer (pH 8.0) containing 5 mM $CaCl_2$ for about 18 h at 37°C and stained with 1% Coomassie brilliant blue R-250. The gelatinolytic activity was identified as a clear band. Pre-stained molecular-weight markers were used to estimate the molecular weight of MMP-2 (about 62 kDa) and MMP-9 (about 90 kDa). Quantification of the bands were estimated by densitometry with the Aida 2.1 Image® software.

STEREOLOGICAL ESTIMATIONS OF CELLULAR PARAMETERS

For stereology analysis, after transfecting cells with Ctr- or Cav1-siRNAs cells were examined with the probe Nucleator [Schmitz et al., 1999] to obtain unbiased estimates of cellular volume, length, and area by means of the Stereo Investigator system (Stereo Investigator software, Version 9.14© 2010, MicroBrightField Europe, Magdeburg, Germany). A stack of MAC 6000 controller modules (Ludl Electronic Products, Ltd, Hawthorne, NY) was configured to interface a Zeiss microscope with a motorized stage and a MBF color digital camera with a PC workstation. Values of cellular volume, length and area were acquired from 25 cells of each group. Volume and area of each cell were estimated according to the formula $V_N = (4\pi/3) \times 1_n^3$, and $a = \pi l^2$, respectively, where l is the length, V_n, number weighted volume, a, area and n, the number of nucleator estimates.

STATISTICAL ANALYSIS

Data showed in figures are mean values ± SE. Statistical significance was determined by Student's *t*-test and a value of $P < 0.05$ was considered statistically significant. All statistical procedures were performed using the Sigma Plot package version 10.

RESULTS

CAV1 KNOCK DOWN AFFECTS CELL MORPHOLOGY

To silence CAV1 we used three double stranded (ds) small interfering RNA (siRNA) named #538, #542, and #545, which were previously demonstrated to efficiently knock down CAV1 in both EA.hy926 and HUVEC [D'Alessio et al., 2010]. As estimated by immunoblotting and real-time PCR (qPCR) analysis, the efficiency of dsRNA in reducing the expression of CAV1 protein as well as of its mRNA transcript was by more than 80%, as shown in Figure 1A,B. In

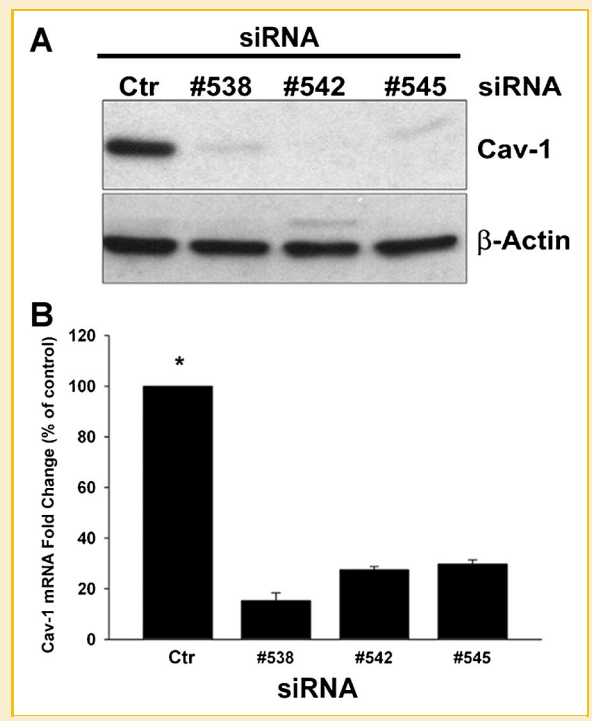

Fig. 1. Effect of CAV1 silencing in EA.hy926 cells. A: CAV1 immunoblotting of total cell lysates showing the efficiency of dsRNA duplex on CAV1 protein expression. β-actin was used as loading control. B: Real-time PCR analysis showing the expression of CAV1 mRNA after transfection of indicated dsRNAs. Ctr indicates control experiment corresponding to cells transfected with the non-targeting dsRNA sequence; $^*P < 0.05$.

addition, qRT-PCR analysis of the expression of the two common cellular stress response genes, namely 2′-5′-oligoadenylate synthetase (OAS) and the protein kinase R (PKR), ruled out the possibility of off-target effect due to dsRNA delivery [Samuel, 2001; Sledz et al., 2003] and revealed that no induction of interferon response following CAV1 dsRNA transfection was observed (data not shown). Morphological analysis of CAV1 silenced cells revealed a significant increase in cell size, when compared with control cells (Fig. 2A). Cell size was further estimated by staining of the actin filament network by using rhodamine-conjugated Phalloidin (Fig. 2B). In addition, the involvement of CAV1 in the regulation of cell size was further evaluated by flow cytometry analysis. As shown in Figure 2C, an increase in the magnitude of forward scatter (FSc-Height), which is roughly proportional to the diameter of the cell, was observed only in the population of cells subjected to CAV1 knock down. In addition, we observed an increase in the magnitude of the side scatter (SSc), which is indicative of structural complexity and granularity inside the cell. Based on these results, we next turned on stereology in order to make a rigorous quantitative and unbiased analysis of a number of three-dimensional cell parameters such as volume, area, and length of the cells, as described in the Materials and Methods Section. Stereological analysis of CAV1 silencing indicated a marked increase of the volume, area, and at a lesser extent of the length of the cells compared with the control cells (Fig. 2D–F), suggesting that CAV1 might directly contribute to the regulation of cellular size and shape.

CAV1 EXPRESSION ON EC MIGRATION AND ANGIOGENESIS

In order to evaluate whether CAV1 regulated migration capacity of EC, we performed an in vitro scratch assay by creating a straight line (scratch) with a p200 pipet tip on both CAV1 silenced and control confluent EC monolayer, as described in the Materials and Methods Section. The results of these experiments clearly demonstrated that the migration proficiency of EC, described by their ability to repair

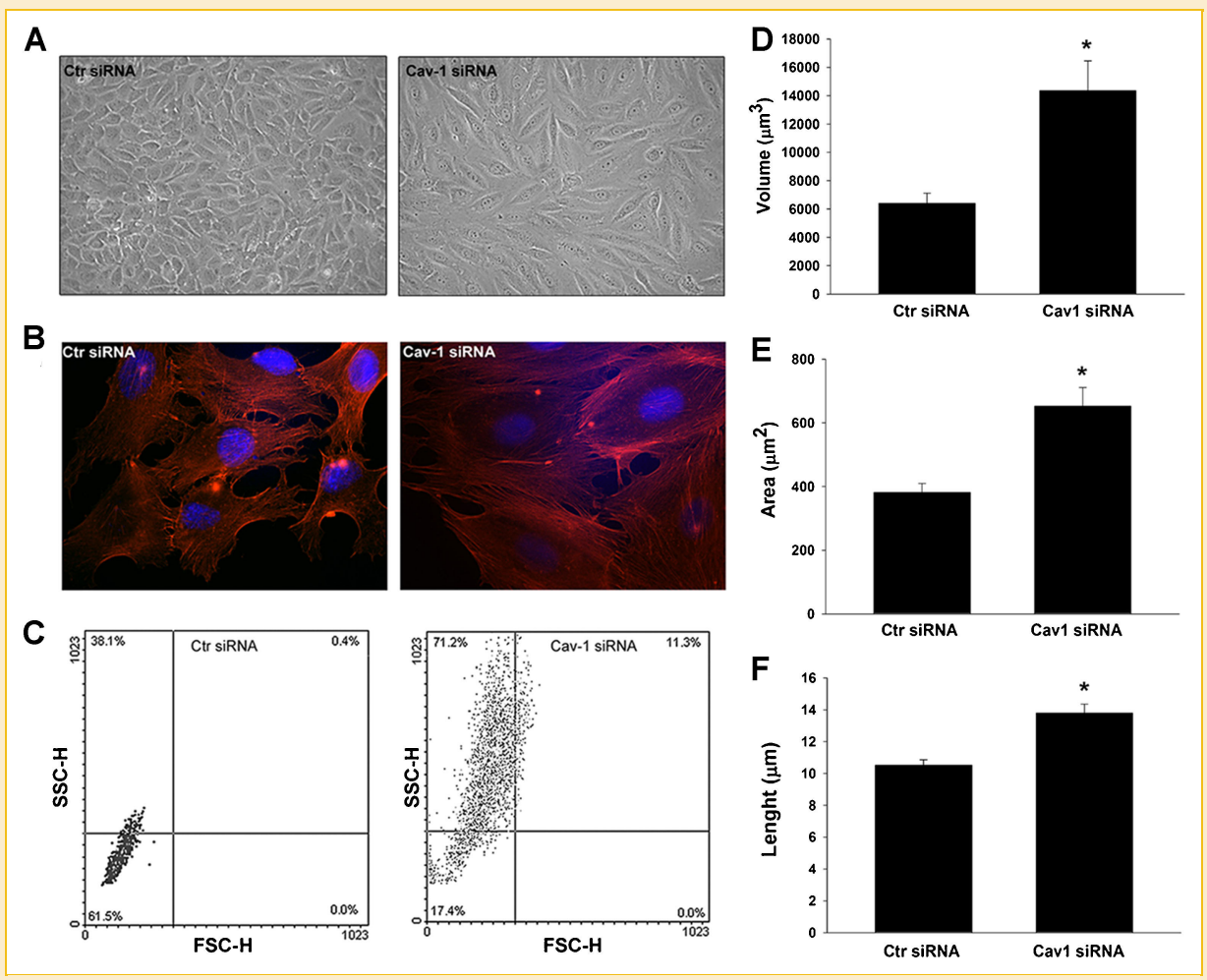

Fig. 2. Morphology and stereology of CAV1 targeted cells. A: Phase contrast microscopy analysis of cells subjected to control and CAV1 dsRNA transfection for 72 h. B: Immunofluorescence microscopy analysis of actin filaments labeled with rhodamine-conjugated phalloidin employed to evaluate the cell size after RNAi. C: Evaluation of forward scatter (FSC-H) and side scatter (SSC-H) by flow cytometric analysis showing increased size and complexity of cells subjected to CAV1 silencing. Data are representative of three independent experiments. D–F: Stereological analysis of volume, area, and length of EC subjected to transfection with the indicated dsRNAs. Error bars in D, E, and F represent SE, N = 3; $^{*}P < 0.01$.

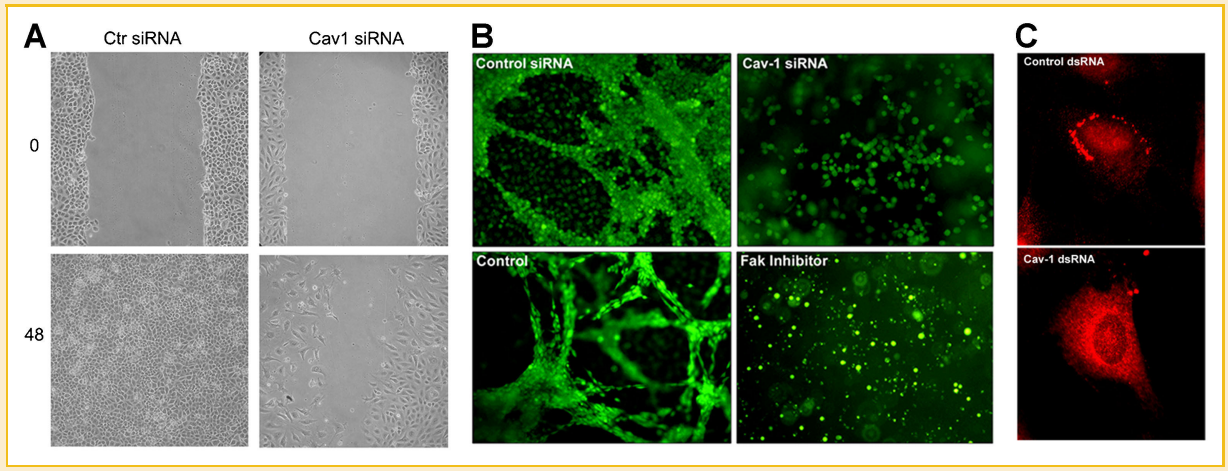

Fig. 3. A: Scratch assay to evaluate the migration capacity of EC subjected to treatment of either control or CAV1 dsRNA at 0 and 48 h. B: In vitro evaluation of VEGF-induced tube formation in siRNA treated cells and in cells incubated with the FAK inhibitor (bottom right) or with vehicle alone (bottom left). C: Immunofluorescence staining of FAK showing the different subcellular distribution of the protein in both control and CAV1 silenced cells.

the wound generated by the tip, was markedly reduced in CAV1 silenced cells when compared to control cells (Fig. 3A). Therefore, to further evaluate the effect of CAV1 on angiogenesis, we performed an in vitro angiogenesis assay by testing the aptitude of CAV1 deficient EC to form tubes on a modified ECM [Hermant et al., 2007] in the presence or absence of 100 ng/ml VEGF. The results of this assay showed that VEGF-induced tube formation was strongly affected in CAV1 silenced cells but not in cells subjected to transfection with the control siRNA in control cells (Fig. 3B). Interestingly, the angiogenic pattern of CAV1 silenced cells appeared to be similar to that seen in cells incubated with the focal adhesion kinase (FAK) inhibitor-14 (Fig. 3B, bottom right panel), which is a key molecule involved in cell proliferation, migration and survival [Schaller, 2010]. These data indicate that CAV1 deficiency might direct affect cell migration and invasion, which are key steps during angiogenesis. To corroborate the contribution of CAV1 to FAK activity, we evaluated the cellular pattern of expression of FAK by means of immunofluorescence staining. CAV1 silenced cells showed a diffused distribution of the FAK protein within the cytoplasm (Fig. 3C), indicating that signaling recruited during angiogenesis requires the proper expression of CAV1 whose absence influenced distribution of FAK and proper movement of EC in the ECM. As angiogenesis is an invasive process which requires proteolytic activities and the remodeling of basement membrane of EC, we next focused on studying MMPs activity such as MMP-2 and MMP-9 [Nalla et al., 2010]. The 72-kDa gelatinase A (MMP-2) is the most widely distributed of all the MMPs and is constitutively expressed by a number of cells, including EC and EA.hy926 cell line [Wu et al., 2005]. By employing the Boyden chamber assay, we found that both basal (serum-induced) and VEGF-induced migration of EC were drastically reduced in CAV1 silenced cells (Fig. 4A). Similarly, CAV1 silencing affected MMP-2 activity, measured by zymography, in both culture medium and cell lysates (Fig. 4B,C). In addition, increasing doses of VEGF failed to induce MMP-2 in CAV1 silenced cells, as indicated in Figure 4D. These findings suggest that CAV1 negatively regulates vascular EC migration mostly by modulating the activity of MMP-2. Moreover, MMP-9, which was less expressed in EA.hy926, appeared unchanged in CAV1 silenced cells (data not shown).

CAV1 KNOCK DOWN AFFECTS CELL CYCLE PROGRESSION AND AKT SIGNAL

Since the increased size displayed by CAV1 targeted cells, we investigated whether this scaffolding protein could affect cell cycle. Therefore, we measured the DNA content of PI-labeled cells passed through a flow cytometer. As shown in Figure 5A, CAV1 silencing induced an increase in G1 phase and a marked reduction of S and G2 phase, indicating the participation of CAV1 in the regulation of cell cycle machinery. These findings correlated to a reduction of cyclin D1, which is required for G1/S transition, and to a diminished phosphorylation of AKT (Fig. 5B), suggesting the involvement of CAV1 in the regulation of AKT pathway. They were also corroborated by the employment of the inhibitor of PI3 kinase, LY294002, which has been extensively used to block PI3 kinase-dependent AKT phosphorylation and kinase activity. As showed in Figure 5C, pretreatment of EC with 5 μM LY294002 for 5 h almost completely prevented VEGF-induced angiogenesis, similarly to what seen in cells deprived of CAV1. LY294002 also affected VEGF-induce ERK activation (Fig. 5C, bottom right panel), supporting a crosstalk between CAV1 and AKT signal. All these data indicate a role of CAV1 in the regulation of cell response to extracellular stimuli (e.g., growth factors) and its possible involvement in the regulation of CDK kinases.

DISCUSSION

This study expands and strengthen our previous findings on the role of the scaffolding protein CAV1 in the regulation of EC functions. By employing specific dsRNAs against the coding sequence of the human CAV1 gene, we showed that the downregulation of this protein affects cell morphology and size, as well as important EC

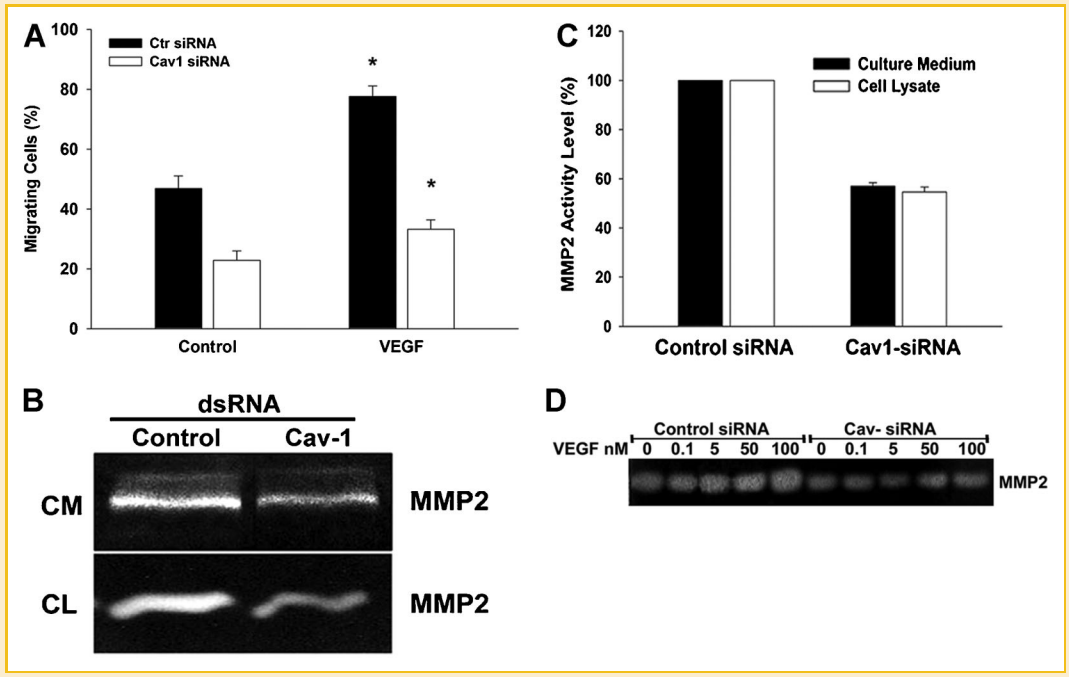

Fig. 4. Effect of CAV1 silencing on cell migration in a modified Boyden chamber assay. A: Cells transfected with either CAV1 siRNA or control siRNA were allowed to migrate for 5 h across the membrane in the Boyden chamber in the presence or absence of 100 ng/ml of VEGF. Cells migrated on the lower surface of the filter were counted in five fields per well. Bars indicate the standard error of three independent experiments. Results are expressed as % of control cell migration; $^{*}P < 0.05$. B: Both conditioned medium and cell lysates from EA.hy926 subjected to transfection with the indicated dsRNA were collected and subjected to gelatin zymography to measure MMP-2 activity. C: Densitometric analysis of serum-induced MMP-2 activity in both culture medium and cell lysates. D: Gelatin zymography of VEGF-induced MMP-2 activity. Data are representative of three independent experiments.

functions such as migration and angiogenesis in the EC line EA.hy926. In particular, silencing of CAV1 induced a marked increase of cell size and complexity as demonstrated by phase contrast microscopy, stress fibers formation, and cytometry. Interestingly, we observed that morphological changes seen in CAV1 silenced cells last as long as 48 h (data not shown). To perform unbiased quantitative estimation of the phenotype observed after CAV1 knock down, we used stereological analysis [Gundersen, 1988], which confirmed a substantial contribution of CAV1 to the regulation of three-dimensional features of the cell. Since the interaction between CAV1 and cholesterol has been extensively reported in the literature, the morphology of CAV1 silenced cells may be related to the deregulation of cellular cholesterol homeostasis [Qi et al., 2009], which is vital for maintaining plasma membrane functions. Since caveolae are specialized version of membrane lipid rafts containing caveolins, it is conceivable that silencing of CAV1 could induce a flattened morphology of these structures making ''measurable'' the portion of plasma membrane masked by invaginated caveolae, therefore increasing the cell surface. In addition, our findings show that silencing of CAV1 induced stress fibers formation which can contribute to the increase of cell size, as previously showed in smooth muscle cells [Romano et al., 2007]. VEGF is a potent angiogenic factor which induces EC proliferation, migration, vascular permeability, and represents an essential survival factor for ECs. We used Boyden chamber migration assay to evaluate the effect of downregulation of CAV1 to EC migration. Our findings show that lowering CAV1 reduces EC migration in both basal condition and in the presence of VEGF. These effects can be explained by the reduced number of caveolae observed after transfection of CAV1 RNAi [D'Alessio et al., 2010]. Silencing of CAV1 might regulate the activity of receptors sequestered in caveolae dampening downstream responses to growth factors detailed in this work (Fig. 6). To this regard, it must be noted that rapid loss of caveolae is normally seen when primary ECs, like HUVEC, are cultivated in vitro [Vasile et al., 1999], which led us to employ EA.hy926 cells that offer an opportunity to investigate the functions that caveolae may play in ECs. In addition, VEGFR2, which mainly transduces VEGF-induced signals, has been shown to be localized within caveolae, supporting a role for caveolae and CAV1 in the activation of VEGF-dependent signals. The effect of CAV1 downregulation also induced a consistent reduction of gelatinase A (MMP-2) which may explain the reduced angiogenic potential in vitro. However, since MMP-9 expression was not significantly modulated by CAV1 downregulation (data not shown), we have confidence that MMP-2 mainly contributes to angiogenesis in a CAV1-dependent manner, at least in EA.hy926. The subcellular distribution of FAK in CAV1 silenced suggests that CAV1 may regulate the proper localization of FAK within focal adhesions, maybe through the interaction with its focal adhesion targeting (FAT) domain [Hildebrand et al., 1993]. Although further studies are needed to understand the molecular mechanism regulating this process, it is possible that CAV1 silencing prevents or at least weakens the binding to the ECM during FAK activation [Parsons et al., 2008]. Most important lack in FAK activation would

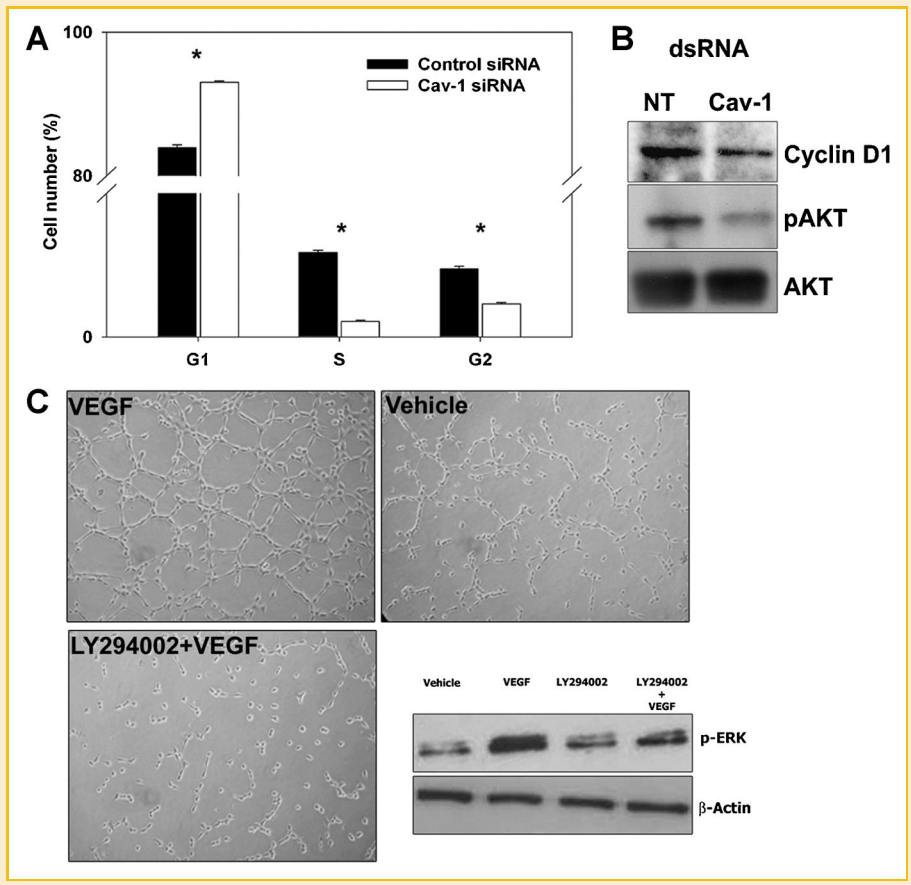

Fig. 5. Analysis of the DNA content in CAV1 silenced cells. A: EA.hy926 were subjected to either control or CAV1 dsRNA transfection for 72 h prior to measure the DNA content by cytofluorometric analysis. B: Immonoblotting analysis of cyclin D1 and phosphorylated (p) AKT in both control and CAV1 silenced cells. Total AKT was used as loading control during SDS–PAGE. C: The effect of the AKT inhibitor, LY294002, on VEGF-induced angiogenesis and ERK activation. Data are representative of three independent experiments; $^{*}P < 0.01$.

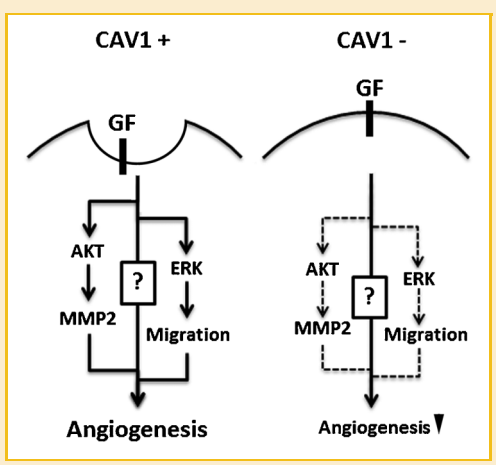

Fig. 6. Schematic model of CAV1 involvement in angiogenesis. Solid and dotted lines indicate activated or reduced pathways in CAV1^{+} or CAV1^{-}, respectively. ?, Depicts other signals involved in angiogenesis; arrowhead indicates reduced angiogenesis, GF, growth factors.

result in the alteration in morphology and migration and angiogenesis. Lowering CAV1 most likely impairs the interaction of the protein with VEGFR2, which can explain changes in AKT activation and influences cell cycle progression. Data presented in this work may also indicate an important role for caveolae as mechanosensing [Spisni et al., 2003; Dupont et al., 2011] structures of EC. Consequently, incorrect expression of CAV1, which is a major caveolae component, can switch the cell to generate uncommon signaling pathways. Finally, although it has been recently discovered that the participation of CAV1 to specific cell functions can be dissociated from its role during caveolae formation [Bernatchez et al., 2011], the specific role of caveolae and caveolins in the regulation of cellular functions has been not fully elucidated and other molecules such as PTRF/cavin-1 may work in concert with CAV1 [Hill et al., 2008], making challenging to understand how caveolae and caveolins regulate disparate cellular signals.

ACKNOWLEDGMENTS

This work was supported by grants from Ministero dell'Università e della Ricerca (MIUR), "Rientro dei Cervelli" Program to A.D. and from Fondazione Roma to E.Z.

REFERENCES

Bai L, Deng X, Li Q, Wang M, An W, Deli A, Gao Z, Xie Y, Dai Y, Cong YS. 2012. Down-regulation of the cavin family proteins in breast cancer. J Cell Biochem 113:322–328.

Bernatchez P, Sharma A, Bauer PM, Marin E, Sessa WC. 2011. A noninhibitory mutant of the caveolin-1 scaffolding domain enhances eNOS-derived NO synthesis and vasodilation in mice. J Clin Invest 121:3747–3755.

Burgermeister E, Liscovitch M, Rocken C, Schmid RM, Ebert MP. 2008. Caveats of caveolin-1 in cancer progression. Cancer Lett 268:187–201.

Chidlow JH, Jr., Sessa WC. 2010. Caveolae, caveolins, and cavins: Complex control of cellular signalling and inflammation. Cardiovasc Res 86: 219–225.

D'Alessio A, Al-Lamki RS, Bradley JR, Pober JS. 2005. Caveolae participate in tumor necrosis factor receptor 1 signaling and internalization in a human endothelial cell line. Am J Pathol 166:1273–1282.

D'Alessio A, Kluger MS, Li JH, Al-Lamki R, Bradley JR, Pober JS. 2010. Targeting of tumor necrosis factor receptor 1 to low density plasma membrane domains in human endothelial cells. J Biol Chem 285: 23868–23879.

Dupont S, Morsut L, Aragona M, Enzo E, Giulitti S, Cordenonsi M, Zanconato F, Le Digabel J, Forcato M, Bicciato S, Elvassore N, Piccolo S. 2011. Role of YAP/TAZ in mechanotransduction. Nature 474:179–183.

Edgell CJ, McDonald CC, Graham JB. 1983. Permanent cell line expressing human factor VIII-related antigen established by hybridization. Proc Natl Acad Sci USA 80:3734–3737.

Feng X, Gaeta ML, Madge LA, Yang JH, Bradley JR, Pober JS. 2001. Caveolin-1 associates with TRAF2 to form a complex that is recruited to tumor necrosis factor receptors. J Biol Chem 276:8341–8349.

Fernandez-Rojo MA, Restall C, Ferguson C, Martel N, Martin S, Bosch M, Kassan A, Leong GM, Martin SD, McGee SL, Muscat GE, Anderson RL, Enrich C, Pol A, Parton RG. 2012. Caveolin-1 orchestrates the balance between glucose and lipid-dependent energy metabolism: Implications for liver regeneration. Hepatology 55:1574–1584.

Gambara G, Billington RA, Debidda M, D'Alessio A, Palombi F, Ziparo E, Genazzani AA, Filippini A. 2008. NAADP-induced Ca(2+) signaling in response to endothelin is via the receptor subtype B and requires the integrity of lipid rafts/caveolae. J Cell Physiol 216:396–404.

Gazzerro E, Sotgia F, Bruno C, Lisanti MP, Minetti C. 2010. Caveolinopathies: From the biology of caveolin-3 to human diseases. Eur J Hum Genet 18:137–145.

Glenney JR, Jr., Soppet D. 1992. Sequence and expression of caveolin, a protein component of caveolae plasma membrane domains phosphorylated on tyrosine in Rous sarcoma virus-transformed fibroblasts. Proc Natl Acad Sci USA 89:10517–10521.

Gundersen HJ. 1988. The nucleator. J Microsc 151:3–21.

Hansen CG, Nichols BJ. 2010. Exploring the caves: Cavins, caveolins and caveolae. Trends Cell Biol 20:177–186.

Hermant B, Desroches-Castan A, Dubessay ML, Prandini MH, Huber P, Vittet D. 2007. Development of a one-step embryonic stem cell-based assay for the screening of sprouting angiogenesis. BMC Biotechnol 7:20.

Hildebrand JD, Schaller MD, Parsons JT. 1993. Identification of sequences required for the efficient localization of the focal adhesion kinase, pp125FAK, to cellular focal adhesions. J Cell Biol 123:993–1005.

Hill MM, Bastiani M, Luetterforst R, Kirkham M, Kirkham A, Nixon SJ, Walser P, Abankwa D, Oorschot VM, Martin S, Hancock JF, Parton RG. 2008. PTRF-Cavin, a conserved cytoplasmic protein required for caveola formation and function. Cell 132:113–124.

Kerbel R, Folkman J. 2002. Clinical translation of angiogenesis inhibitors. Nat Rev Cancer 2:727–739.

Liang CC, Park AY, Guan JL. 2007. In vitro scratch assay: A convenient and inexpensive method for analysis of cell migration in vitro. Nat Protoc 2: 329–333.

Livak KJ, Schmittgen TD. 2001. Analysis of relative gene expression data using real-time quantitative PCR and the 2(-Delta Delta C(T)) method. Methods 25:402–408.

Nalla AK, Gorantla B, Gondi CS, Lakka SS, Rao JS. 2010. Targeting MMP-9, uPAR, and cathepsin B inhibits invasion, migration and activates apoptosis in prostate cancer cells. Cancer Gene Ther 17:599–613.

Newby AC. 2012. Matrix metalloproteinase inhibition therapy for vascular diseases. Vascul Pharmacol 56:232–244.

Parsons JT, Slack-Davis J, Tilghman R, Roberts WG. 2008. Focal adhesion kinase: Targeting adhesion signaling pathways for therapeutic intervention. Clin Cancer Res 14:627–632.

Parton RG, Simons K. 2007. The multiple faces of caveolae. Nat Rev Mol Cell Biol 8:185–194.

Pober JS, Sessa WC. 2007. Evolving functions of endothelial cells in inflammation. Nat Rev Immunol 7:803–815.

Qi M, Liu Y, Freeman MR, Solomon KR. 2009. Cholesterol-regulated stress fiber formation. J Cell Biochem 106:1031–1040.

Quest AF, Lobos-Gonzalez L, Nunez S, Sanhueza C, Fernandez JG, Aguirre A, Rodriguez D, Leyton L, Torres V. 2012. The caveolin-1 connection to cell death and survival. Curr Mol Med 13:266–281.

Reglero-Real N, Marcos-Ramiro B, Millan J. 2012. Endothelial membrane reorganization during leukocyte extravasation. Cell Mol Life Sci 69:3079–3099.

Romano F, Gambara G, De Cesaris P, Ziparo E, Palombi F, Filippini A. 2007. Endothelin induces functional hypertrophy of peritubular smooth muscle cells. J Cell Physiol 212:264–273.

Roy UK, Henkhaus RS, Loupakis F, Cremolini C, Gerner EW, Ignatenko NA. 2013. Caveolin-1 is a novel regulator of K-RAS-dependent migration in colon carcinogenesis. Int J Cancer. DOI: 10.1002/ijc.28001

Samuel CE. 2001. Antiviral actions of interferons. Clin Microbiol Rev 14:778–809.

Schaller MD. 2010. Cellular functions of FAK kinases: Insight into molecular mechanisms and novel functions. J Cell Sci 123:1007–1013.

Scherer PE, Okamoto T, Chun M, Nishimoto I, Lodish HF, Lisanti MP. 1996. Identification, sequence, and expression of caveolin-2 defines a caveolin gene family. Proc Natl Acad Sci USA 93:131–135.

Schmitz C, Schuster D, Niessen P, Korr H. 1999. No difference between estimated mean nuclear volumes of various types of neurons in the mouse brain obtained on either isotropic uniform random sections or conventional frontal or sagittal sections. J Neurosci Methods 88:71–82.

Sengupta D. 2012. Cholesterol modulates the structure, binding modes, and energetics of caveolin-membrane interactions. J Phys Chem B 116:14556–14564.

Sledz CA, Holko M, de Veer MJ, Silverman RH, Williams BRG. 2003. Activation of the interferon system by short-interfering RNAs. Nat Cell Biol 5:834–839.

Song KS, Scherer PE, Tang Z, Okamoto T, Li S, Chafel M, Chu C, Kohtz DS, Lisanti MP. 1996. Expression of caveolin-3 in skeletal, cardiac, and smooth muscle cells. Caveolin-3 is a component of the sarcolemma and co-fractionates with dystrophin and dystrophin-associated glycoproteins. J Biol Chem 271:15160–15165.

Spisni E, Bianco MC, Griffoni C, Toni M, D'Angelo R, Santi S, Riccio M, Tomasi V. 2003. Mechanosensing role of caveolae and caveolar constituents in human endothelial cells. J Cell Physiol 197:198–204.

Stetler-Stevenson WG. 1999. Matrix metalloproteinases in angiogenesis: A moving target for therapeutic intervention. J Clin Invest 103:1237–1241.

Thiele C, Hannah MJ, Fahrenholz F, Huttner WB. 2000. Cholesterol binds to synaptophysin and is required for biogenesis of synaptic vesicles. Nat Cell Biol 2:42–49.

Vasile E, Qu H, Dvorak HF, Dvorak AM. 1999. Caveolae and vesiculo-vacuolar organelles in bovine capillary endothelial cells cultured with VPF/VEGF on floating Matrigel-collagen gels. J Histochem Cytochem 47:159–167.

Wu H-T, Lin S-H, Chen Y-H. 2005. Inhibition of cell proliferation and in vitro markers of angiogenesis by indole-3-carbinol, a major indole metabolite present in cruciferous vegetables. J Agric Food Chem 53:5164–5169.